

Supplementary Materials for Detecting Non-Markovianity via Quantified Coherence: Theory and Experiments

Kang-Da Wu,^{1,2} Zhibo Hou,^{1,2} Guo-Yong Xiang,^{1,2,*} Chuan-Feng
Li,^{1,2} Guang-Can Guo,^{1,2} Daoyi Dong,³ and Franco Nori^{4,5}

¹CAS Key Laboratory of Quantum Information, University of Science and Technology of China, Hefei, 230026, People's Republic of China

²CAS Center For Excellence in Quantum Information and Quantum Physics,
University of Science and Technology of China, Hefei, 230026, People's Republic of China

³School of Engineering and Information Technology, University of New South Wales, Canberra, ACT, 2600, Australia

⁴Theoretical Quantum Physics Laboratory, RIKEN Cluster for Pioneering Research, Wako-shi, Saitama 351-0198, Japan

⁵Physics Department, University of Michigan, Ann Arbor Michigan 48109-1040, USA

(Dated: February 6, 2020)

S1. THEORETICAL TOOLS

A *quantum resource theory* (QRT) has several indispensable ingredients, including: constraints, states which contain no resource, and a measure for how much resource a state possesses. The constraints, known as free operations, in a QRT are often desirable from a practical perspective that reflects current experimental capabilities. The states that contain no resource are often referred to as free states, and these can be generated by free operations without any cost. In the following, let us first briefly recall some basic information about free states and free operations in coherence theory.

A. Free states in the resource theory of quantum coherence

The free states in the resource theory of quantum coherence are incoherent states [1]. A quantum state ρ is said to be incoherent in a given reference basis $\{|i\rangle\}$ if that state is diagonal in this basis, i.e.,

$$\rho = \sum_i p_i |i\rangle\langle i|, \quad (\text{S1})$$

where $0 \leq p_i \leq 1$, for all i , and $\sum_i p_i = 1$. The reference basis is often chosen according to the context of the story, usually motivated by physical grounds of being easy to synthesize or store, e.g., eigenbasis of the Hamiltonian in quantum thermodynamics, polarization or path degree of a photon, internal states of an ionic atom, and so on.

For bipartite systems partitioned by A and B , each with respective local reference bases $\{|i\rangle^A\}$ and $\{|j\rangle^B\}$, the incoherent states take the form

$$\chi^{AB} = \sum_{ij} p_{ij} |i\rangle\langle i|^A \otimes |j\rangle\langle j|^B, \quad (\text{S2})$$

where $0 \leq p_{ij} \leq 1$, and $\sum_{ij} p_{ij} = 1$. Note that in the aforementioned bipartite systems, we can also choose an orthogonal complete set of entangled pure states as the reference basis. In this case, the bipartite systems are viewed as a single physical system.

In the above case, coherence in both A and B are viewed as resources. In the task of *assisted distillation of quantum coherence* [2], involving a bipartite system (Alice and Bob) where only the coherence of Bob is viewed as a resource, the *quantum-incoherent (QI)* states are introduced and can be regarded as free states,

$$\chi^{AB} = \sum_i p_i \sigma_i^A \otimes |i\rangle\langle i|^B. \quad (\text{S3})$$

Here, σ_i^A is an arbitrary quantum state on Alice's side and the state $|i\rangle^B$ belongs to the local incoherent basis of Bob.

B. Quantification of quantum coherence in single and bipartite systems

Several coherence measures have been proposed, for quantifying the degree of coherence in both single systems and bipartite systems.

Regarding the degree of coherence in a single system, we adopt the most popular quantifier: the *relative entropy of coherence* (REC). The REC captures how far a given state ρ is from the set of incoherent states,

$$C_r(\rho) = \min_{\chi \in \mathcal{I}} S(\rho \|\chi), \quad (\text{S4})$$

where $S(\rho \|\chi)$ denotes the *relative entropy* between two quantum states ρ and χ ,

$$S(\rho \|\chi) = \text{Tr}(\rho \log_2 \rho - \rho \log_2 \chi), \quad (\text{S5})$$

and the minimization in Eq. (S4) is taken over all incoherent states. Another representation of REC is

$$C_r(\rho) = S[\Delta(\rho)] - S(\rho), \quad (\text{S6})$$

where Δ denotes the dephasing operation in the incoherent basis, and $S(\rho)$ denotes the von Neumann entropy of a quantum state ρ ,

$$S(\rho) = -\text{Tr}(\rho \log_2 \rho). \quad (\text{S7})$$

The REC has operational significance as it equals the *distillable coherence* (DC) C_d [3],

$$C_d(\rho) = \sup \left\{ R : \lim_{n \rightarrow \infty} \left(\inf_{\Lambda} \|\Lambda[\rho^{\otimes n}] - \Phi_2^{\otimes \lfloor Rn \rfloor}\| \right) = 0 \right\}, \quad (\text{S8})$$

where, $\|A\| = \text{Tr} \sqrt{A^\dagger A}$ is the trace norm, and the infimum is taken over all incoherent operations Λ . Similar to the entanglement distillation, general quantum states ρ can be used for asymptotic distillation of maximally coherent states via incoherent operations.

Regarding the quantification of coherence on one subsystem in a bipartite system, the *quantum-incoherent relative entropy of coherence* (*QI REC*) is defined as [2]

$$C_r^{A|B}(\rho^{AB}) = \min_{\chi^{A|B} \in \mathcal{I}^{A|B}} S(\rho^{AB} \|\chi^{A|B}), \quad (\text{S9})$$

where the minimum is taken over the set of *QI* states. The *QI REC* $C_r^{A|B}$ captures *how close a quantum state is from the set of QI states*. Another expression is [2]

$$C_r^{A|B}(\rho^{AB}) = S[\Delta^B(\rho^{AB})] - S(\rho^{AB}), \quad (\text{S10})$$

where Δ^B denotes dephasing in the incoherent basis of Bob.

C. Free operations in the resource theory of quantum coherence

The free operations in the QRT of coherence in a single system are operations that do not create coherence from incoherent states,

$$\Lambda(\rho) \in \mathcal{I}, \quad \forall \rho \in \mathcal{I}, \quad (\text{S11})$$

where \mathcal{I} denotes the set of incoherent states. Such operations constitute the largest possible set that are free and referred to as *maximally incoherent operations*. One subset of such free operations are incoherent operations, which were first introduced in [1], specified by a set of Kraus operators $\{K_n\}$, satisfying that each of its Kraus operators is incoherent,

$$K_n \mathcal{I} K_n^\dagger \subset \mathcal{I}^*, \quad \forall n, \quad (\text{S12})$$

where \mathcal{I}^* denotes the set of diagonal semi-definite Hermitian operators. A general *completely positive and trace preserving* (CPTP) map Λ is incoherent if there exists at least one incoherent Kraus representation. Then the *dephasing-covariant incoherent operations* (DIO) are maps Λ which commute with the dephasing operation Δ , i.e., $\Delta[\Lambda(\rho)] =$

$\Lambda[\Delta(\rho)]$. And finally, the *strictly incoherent operations* form the smallest set of free operations, where both K_n and K_n^\dagger are incoherent operators.

Regarding the resource theory of coherence in a bipartite scenario, where the coherence of one subsystem is viewed as resource, the *local quantum-incoherent operations and classical communications* (LQICC) protocol was first introduced in [2]. In a bipartite system involving Alice and Bob, Bob is restricted to perform only local incoherent operations while Alice can perform arbitrary quantum operations on her system. Classical communications between them are allowed. The *QI REC* has the operational meaning that it upper bounds the optimal generation rate of the maximally coherent state $|\Phi_2\rangle$ on Bob's side in the LQICC protocol. The *distillable coherence of collaboration* (DCC) was first introduced in [2],

$$C_d^{AB}(\rho^{AB}) = \sup \left\{ R : \lim_{n \rightarrow \infty} \left(\inf_{\Lambda} \|\Lambda \left[(\rho^{AB})^{\otimes n} \right] - \Phi_2^{\otimes \lfloor Rn \rfloor}\| \right) = 0 \right\}, \quad (\text{S13})$$

where the infimum is taken over all LQICC operations Λ and $\lfloor x \rfloor$ returns the maximum integer no larger than x . This quantity is upper bounded by $C_r^{AB}(\rho^{AB})$ for general mixed quantum states ρ^{AB} , and the equality can be achieved for pure bipartite resource state $|\Phi\rangle^{AB}$ and specific class of mixed states like maximally correlated states. But for general states, like Werner states, the upper bound cannot be reached.

D. Relation between the QI relative entropy of coherence and the steering induced coherence

First we introduce a relation between the *QI REC* and the *steering induced coherence* (SIC).

Proposition 1—For a bipartite state ρ^{AB} , the SIC is upper bounded by the *QI REC*; i.e., we have

$$C_r^{AB}(\rho^{AB}) \geq \bar{C}_r^B(\rho^{AB}). \quad (\text{S14})$$

Proof—Note that the *QI REC* can be expressed as

$$C_r^{AB}(\rho^{AB}) = \min_{\chi^{AB} \in \mathcal{I}^{AB}} S(\rho^{AB} \|\chi^{AB}) = S[\rho^{AB} \|\Delta^B(\rho^{AB})]. \quad (\text{S15})$$

Recall that the quantum relative entropy has many important properties, such that [4, 5]:

$$(a) \quad S[\Lambda(\rho) \|\Lambda(\sigma)] \leq S(\rho \|\sigma), \quad (\text{S16a})$$

$$(b) \quad \sum_i p_i S(K_i \rho K_i^\dagger / p_i \|\ K_i \sigma K_i^\dagger / q_i) \leq \sum_i S(K_i \rho K_i^\dagger \|\ K_i \sigma K_i^\dagger), \quad (\text{S16b})$$

$$(c) \quad S\left(\sum_i P_i \rho P_i \|\ \sum_i P_i \sigma P_i\right) = \sum_i S(P_i \rho P_i \|\ P_i \sigma P_i), \quad (\text{S16c})$$

$$(d) \quad S(P_i \otimes \rho \|\ P_i \otimes \sigma) = S(\rho \|\sigma), \quad (\text{S16d})$$

$$(e) \quad S(\text{Tr}_p \rho \|\ \text{Tr}_p \sigma) \leq S(\rho \|\sigma) \quad (\text{S16e})$$

where $p_i = \text{Tr}(K_i \rho K_i^\dagger)$, $q_i = \text{Tr}(K_i \sigma K_i^\dagger)$, and $\{P_i\}$ is a set of orthogonal projectors.

Note that $\{\mathbf{M}_n^A\}$ is a set of local measurement operators on Alice's system, corresponding to the measurement outcome n . Thus with property (a) in Eq. (S16), we have

$$C_r^{AB}(\rho^{AB}) = S[\rho^{AB} \|\Delta^B(\rho^{AB})] \geq S\left[\sum_n \mathbf{M}_n^A \rho^{AB} (\mathbf{M}_n^A)^\dagger \|\ \sum_n \mathbf{M}_n^A \Delta^B(\rho^{AB}) (\mathbf{M}_n^A)^\dagger\right]. \quad (\text{S17})$$

Following (b) in Eq. (S16) and [5], if we denote $\delta_n^B = \text{Tr}_A \mathbf{M}_n^A \rho^{AB} (\mathbf{M}_n^A)^\dagger$, $p_n = \text{Tr}(\delta_n^B)$, and $\rho_n^B = \frac{\delta_n^B}{p_n}$, we have

$$S\left[\sum_n \mathbf{M}_n^A \rho^{AB} (\mathbf{M}_n^A)^\dagger \|\ \sum_n \mathbf{M}_n^A \Delta^B(\rho^{AB}) (\mathbf{M}_n^A)^\dagger\right] \geq \sum_n p_n S\left[\mathbf{M}_n^A \rho^{AB} (\mathbf{M}_n^A)^\dagger / p_n \|\ \mathbf{M}_n^A \Delta^B(\rho^{AB}) (\mathbf{M}_n^A)^\dagger / q_n\right]. \quad (\text{S18})$$

Then with property (e) in Eq. (S16), we can obtain

$$\sum_n p_n S \left[\mathbf{M}_n^A \rho^{AB} (\mathbf{M}_n^A)^\dagger / p_n \parallel \mathbf{M}_n^A \Delta^B (\rho^{AB}) (\mathbf{M}_n^A)^\dagger / q_n \right] \geq \sum_n p_n S \left[\rho_n^B \parallel \Delta^B (\rho_n^B) \right] = \sum_n p_n C_r^B (\rho_n^B). \quad (\text{S19})$$

Note that $\sum_n p_n C_r^B (\rho_n^B)$ is the average coherence that Bob can obtain with Alice's measurement choice $\{\mathbf{M}_n^A\}$ and classical communications. No matter what measurement Alice actually chooses, Bob will reach an average coherence no greater than $C_r^{AB} (\rho^{AB})$. Hence, we have $C_r^{AB} (\rho^{AB}) \geq \bar{C}_r^B (\rho^{AB})$.

E. Difference between the QI relative entropy of coherence and quantum correlations

Note that the QI REC is essentially different from the measures of quantum correlations. First, any state that is not quantum-incoherent has nonzero QI REC. The difference between the measures of quantum correlations and the QI REC is that the latter is basis-dependent. One of the most popular measures of quantum correlations is the *relative entropy of quantum discord* [6–8], defined as

$$D(\rho^{AB}) = \min_{\delta^{AB} \in CC} S(\rho^{AB} \parallel \delta^{AB}) \quad (\text{S20})$$

where CC denotes the set of *classical correlated states* that can be written in the form of the sum of projectors

$$\delta^{AB} = \sum_{k,l} p_{kl} |k\rangle\langle k|^A \otimes |l\rangle\langle l|^B. \quad (\text{S21})$$

Now consider a family of bipartite states

$$f^{AB} = \sum_{k,m} p_{km} |k\rangle\langle k|^A \otimes |m\rangle\langle m|^B, \quad (\text{S22})$$

where $|k\rangle^A$ is any orthonormal basis of Alice, and $|m\rangle^B$ is any orthonormal basis of Bob that is not incoherent. Obviously, f^{AB} is not quantum-incoherent and thus has a nonzero QI REC, while f^{AB} has zero discord or entanglement. Moreover, we can also construct states that are quantum-incoherent but have nonzero quantum discord.

F. Concurrence

The concurrence is an entanglement monotone, defined for a mixed state of two qubits as:

$$E_c^{AB}(\rho) \equiv \max(0, \lambda_1 - \lambda_2 - \lambda_3 - \lambda_4), \quad (\text{S23})$$

where $\lambda_1, \dots, \lambda_4$ are the eigenvalues of the Hermitian matrix $R = \sqrt{\sqrt{\rho} \tilde{\rho} \sqrt{\rho}}$, with

$$\tilde{\rho} = (\sigma_y \otimes \sigma_y) \rho^* (\sigma_y \otimes \sigma_y), \quad (\text{S24})$$

where ρ^* denotes the spin-flipped state of ρ , σ_y a Pauli spin matrix, and the eigenvalues are listed in decreasing order.

S2. DYNAMICAL BEHAVIORS OF THE INFORMATION CARRIERS BASED ON COHERENCE IN OPEN SYSTEMS: THEORETICAL PROOF

Proof of Lemma 1—The family of IOSDs will preserve incoherent states; i.e., for each $\rho \in \mathcal{I}$, we have

$$\Lambda_t(\rho) \in \mathcal{I}, \quad (\text{S25})$$

for any $t \geq 0$. Let us denote the quantum states after evolution time s and t ($0 \leq s \leq t$) are ρ_s and ρ_t . Then the REC of ρ_t and ρ_s can be evaluated as

$$C_r(\rho_t) = S[\rho_t \parallel \Delta(\rho_t)], \quad (\text{S26a})$$

$$C_r(\rho_s) = S[\rho_s \parallel \Delta(\rho_s)]. \quad (\text{S26b})$$

Note that if $\{\Lambda_t\}$ is Markovian, we have $\Lambda_t = \Lambda_{t,s}\Lambda_{s,0}$, and $\Lambda_{t,s}$ is CPTP. Hence, we can use the relation

$$S[\rho_t \|\Delta(\rho_t)] \leq S[\Lambda_{t,s}(\rho_s) \|\Lambda_{t,s}\Delta(\rho_s)], \quad (\text{S27})$$

and the definition of coherence measure yields

$$C_r(\rho_t) = \min_{\delta_t \in \mathcal{I}} S[\rho_t \|\delta_t] \leq S[\rho_t \|\Lambda_{t,s}\Delta(\rho_s)]. \quad (\text{S28})$$

Then we can obtain

$$C_r(\rho_t) \leq S[\Lambda_{t,s}(\rho_s) \|\Lambda_{t,s}\Delta(\rho_s)] \leq C_r(\rho_s). \quad (\text{S29})$$

We have also used the property in Eq. (S16) that the quantum relative entropy is contractive under CPTP maps. Thus we complete the proof.

Proof of Lemma 2—Following [9] and the proof of Lemma 1, with

$$C_r(\rho_t^{AB}) = S[\rho_t^{AB} \|\Delta^{AB}(\rho_t^{AB})], \quad (\text{S30a})$$

$$C_r(\rho_s^{AB}) = S[\rho_s^{AB} \|\Delta^{AB}(\rho_s^{AB})], \quad (\text{S30b})$$

we have

$$C_r(\rho_t^{AB}) \leq S[\Lambda_{t,s}^A(\rho_s^{AB}) \|\Lambda_{t,s}^A\Delta^{AB}(\rho_s^{AB})] \leq C_r(\rho_s^{AB}). \quad (\text{S31})$$

Thus we see the dynamical behavior of the extended coherence during an IOSD.

From the above two Lemmas, we can see that both the coherence of the open system and the extended coherence of the open system and the ancilla decrease monotonically during an IOSD, and they can be used for *efficiently detecting non-Markovianity in IOSDs*. However, there are dynamics that are not incoherent. Hence, both of these information carriers will not decrease monotonically in these processes. We then prove *Theorem 1*, showing the monotonic behaviors of the *QI* REC during general open system dynamics.

Proof of Theorem 1—First we prove that the *QI* REC decreases monotonically during a Markovian evolution on Alice. The quantum states (initially ρ^{AB}) after evolution time s and t ($0 \leq s \leq t$) are ρ_s^{AB} and ρ_t^{AB} . We can express the *QI* REC as follows,

$$C_r^{AB}(\rho_t^{AB}) = S[\rho_t^{AB} \|\Delta^B(\rho_t^{AB})] = S[\Lambda_{t,s}^A(\rho_s^{AB}) \|\Delta^B \Lambda_{t,s}^A(\rho_s^{AB})]. \quad (\text{S32})$$

As Δ^B acts only on B , and $\Lambda_{t,s}^A$ acts only on A , we have

$$\Delta^B \Lambda_{t,s}^A(\cdot) = \Lambda_{t,s}^A \Delta^B(\cdot). \quad (\text{S33})$$

Combining the contractive property, if the intermediate map $\Lambda_{t,s}^A$ is CP, we have

$$S[\rho_t^{AB} \|\Delta^B(\rho_t^{AB})] \leq S[\rho_s^{AB} \|\Delta^B(\rho_s^{AB})]. \quad (\text{S34})$$

Thus during a Markovian process, the *QI* REC decreases monotonically.

Proof of Theorem 2—Then we prove that the SIC decreases monotonically during a Markovian evolution on Alice. It is well known that any CPTP operation on Alice can be constructed by first implementing a unitary U to A and an ancilla A' , then discarding A' . The corresponding mathematical formulation can be described by

$$\Lambda(\rho^A) = \text{Tr}_{A'}[U(\rho^A \otimes \rho^{A'})U^\dagger], \quad (\text{S35})$$

where ρ^A and $\rho^{A'}$ denote the quantum states of A and A' .

Note that if Bob shares a multipartite state $\rho^{A_1 \dots A_n B}$ made of n parties A_1, A_n, \dots, A_n , the generalized steering-induced coherence can be expressed as

$$\bar{C}_r^B(\rho^{A_1 \dots A_n B}) = \max_{\mathcal{M}_{A_1 \dots A_n}} \sum_m p_m C_r(\rho_m^B), \quad (\text{S36})$$

where $\mathcal{M}_{A_1 \dots A_n}$ denotes the collective measurements across n particles. In our case, Alice (A), Bob and the ancilla A' share a tripartite state before the unitary U , where A and A' are uncorrelated. The overall state admits the form

$$\rho^{A'AB} = \rho^{A'} \otimes \rho^{AB}. \quad (\text{S37})$$

As any collective measurement on A and A' will reduce to a *positive-operator valued measure* (POVM) on A , and the set of all collective measurements on AA' forms a strict larger set than the set of all local measurements, yielding higher average coherence that can be obtained on Bob's system in general. Thus, we obtain the following relation,

$$\bar{C}_r^B(\rho^{A'AB}) = \max_{\mathcal{M}_{AA'}} \sum_m p_m C_r(\rho_m^B) \geq \bar{C}_r^B(\rho^{AB}). \quad (\text{S38})$$

The above inequality is valid in a more general case when A and A' are correlated. However, in the case when A' and A are product states, we have

$$\bar{C}_r^B(\rho^{A'AB}) = \bar{C}_r^B(\rho^{AB}). \quad (\text{S39})$$

First we present the proof of this statement. Consider a collective measurement, specified by

$$\{\mathcal{M}_{A'A}^k = \sum_i s_i^k |s_i^k\rangle\langle s_i^k|\}, \quad (\text{S40})$$

which acts on A and A' , where $\{|s_i^k\rangle\}$ and $\{|s_i^k\rangle\}$ are the eigenvalues and eigenvectors of $\mathcal{M}_{A'A}^k$. The normalization condition leads to

$$\sum_k \mathcal{M}_{A'A}^k = \mathbb{I}, \quad (\text{S41})$$

where \mathbb{I} denotes the identity operator on A and A' . The reduced POVM on A satisfies

$$\text{Tr}(\mathcal{M}_A^k \rho^A) = \text{Tr}(\mathcal{M}_{A'A}^k \rho^{A'} \otimes \rho^A). \quad (\text{S42})$$

Here M_A^k denotes a local measurement operator corresponding to k , which can be constructed by

$$M_A^k = \sum_{a',i} s_i^k \langle a' | s_i^k \rangle \langle s_i^k | \rho^{A'} | a' \rangle, \quad (\text{S43})$$

which corresponds to the auxiliary state $\rho^{A'}$, and $|a'\rangle$ denotes orthogonal basis on A' . Then after implementing the POVM, Bob can obtain the state ρ_k^B from according to each M_A^k . The state of Bob can be expressed as

$$\rho_k^B = \frac{\text{Tr}_A M_A^k \rho^{AB}}{\text{Tr}_{AB} M_A^k \rho^{AB}}. \quad (\text{S44})$$

Denoting $p_k = \text{Tr}_{AB} M_A^k \rho^{AB}$, the average coherence obtained by Bob after the implementation of the POVM can be expressed as

$$\bar{C}_r^B(\rho^{AB} | \mathcal{M}_A) = \sum_k p_k C_r^B(\rho_k^B). \quad (\text{S45})$$

If we denote the state $\rho_{kl|AA'}$ as Bob's state after Alice's and the ancilla's measurement $M_{AA'}^k$, then we have

$$\rho_{kl|AA'}^B = \frac{\text{Tr}_{AA'} \sum_i s_i^k |s_i^k\rangle\langle s_i^k| \rho^{A'} \otimes \rho^{AB}}{\text{Tr}_{A'AB} \sum_i s_i^k |s_i^k\rangle\langle s_i^k| \rho^{A'} \otimes \rho^{AB}} = \frac{\text{Tr}_A \sum_{i,a'} s_i^k \langle a' | s_i^k \rangle \langle s_i^k | \rho^{A'} | a' \rangle \rho^{AB}}{\text{Tr}_{AB} \sum_{i,a'} s_i^k \langle a' | s_i^k \rangle \langle s_i^k | \rho^{A'} | a' \rangle \rho^{AB}} = \rho_k^B. \quad (\text{S46})$$

We can see that each measurement on AA' can be realized by a measurement on A , while does not change the Bob's steered state.

From this we can see that the average coherence, obtained from any collective measurement on A' and A , is no greater than that is obtained from a proper designed measurement on A if A and A' are product states. After the

CPTP operation on A , which is realized by the unitary on A' and A , the maximum of the average coherence obtained from the collective measurement remains unchanged, i.e.,

$$\bar{C}_r^B(\rho^{A'AB}) = \bar{C}_r^B(\rho_U^{A'AB}), \quad (\text{S47})$$

where $\rho_U^{A'AB} = U^{AA'} \rho^{A'AB} (U^{AA'})^\dagger$. The average coherence obtained from the collective measurement on A and A' is upper bounded by $\bar{C}_r^B(\rho^{AB})$. After the unitary U , we have

$$\bar{C}_r^B(\rho_U^{A'AB}) = \bar{C}_r^B(\rho^{AB}). \quad (\text{S48})$$

When tracing over A' , the set of measurements on A is a strict subset of the reduced POVMs corresponding to collective measurements on A and A' . Thus, we have

$$\bar{C}_r^B(\rho_U^{AB}) \leq \bar{C}_r^B(\rho_U^{A'AB}), \quad (\text{S49})$$

where ρ_U^{AB} denotes the final states of Alice and Bob after the implementation of U ,

$$\rho_U^{AB} = \text{Tr}_{A'}(\rho_U^{A'AB}). \quad (\text{S50})$$

Using the fact that any CPTP map on A can be constructed by unitary interaction between A and an uncorrelated A' , as denoted in Eq. (S35), the SIC of B will decrease under a CPTP map on A ,

$$\bar{C}_r^B[\Lambda^A(\rho^{AB})] \leq \bar{C}_r^B(\rho^{AB}). \quad (\text{S51})$$

Thus we complete the proof. This result shows that *the Markovianity on Alice's evolution will reduce the steerability of Alice to Bob's state, shrinking the accessible states of Bob*, while the local state of Bob ρ^B will remain unchanged.

S3. NUMERICAL SIMULATIONS FOR DIFFERENT PROCESSES

In this section we present the numerical simulations to show the behaviors of the local coherence of a single system, the extended coherence with an ancilla, the QI REC, and the SIC, under different non-Markovian quantum dynamics. To simulate the behavior of the REC of a single qubit system, we use the initial pure state

$$|\psi_0\rangle^A = \frac{1}{2}(\sqrt{3}|0\rangle + |1\rangle). \quad (\text{S52})$$

And to simulate the dynamical behaviors of the extended coherence with an ancilla, the QI REC, and the SIC on a bipartite system, we choose the initial two-qubit entangled state

$$|\psi_0\rangle^{AB} = \frac{1}{4}(\sqrt{6}|00\rangle + \sqrt{2}|01\rangle + \sqrt{2}|10\rangle + \sqrt{6}|11\rangle). \quad (\text{S53})$$

We consider two kinds of quantum dynamics: the amplitude-damping channels and the multiple decoherence channels.

A. Amplitude-damping channels

We now consider the single-qubit amplitude-damping channels modeled by the Hamiltonian

$$H_{\text{tot}} = \frac{1}{2}\omega_0\sigma_z + \sum_i \omega_i a_i^\dagger a_i + \sum_i (g_i \sigma_+ a_i + g_i^* \sigma_- a_i^\dagger) \quad (\text{S54})$$

where, ω_i denotes frequency of the noise, g_k is the coupling constant, σ_+ and σ_- are the raising and lowering operators for the qubit. The master equation corresponding to the Hamiltonian in Eq. (S54) is given by

$$\frac{d}{dt}\rho_t = -\frac{i}{4}S(t)[\sigma_z, \rho] + \gamma(t)\left(\sigma_- \rho_t \sigma_+ - \frac{1}{2}\{\sigma_+ \rho_t \sigma_- - \rho_t\}\right) \quad (\text{S55})$$

where the quantities $S(t)$ and $\gamma(t)$ read

$$S(t) = -2\text{Im}\frac{\dot{G}(t)}{G(t)}, \quad (\text{S56a})$$

$$\gamma(t) = -2\text{Re}\frac{\dot{G}(t)}{G(t)}, \quad (\text{S56b})$$

and the *decoherence function* $G(t)$ depends on the spectral density $J(\omega)$. Considering a Lorentzian shape spectral density,

$$J(\omega) = \frac{\gamma_0\lambda^2}{[(\omega_0 + \delta - \omega)^2 + \lambda^2]}, \quad (\text{S57})$$

and letting $\delta = 0$, one obtains the decoherence function $G(t)$ as

$$G(t) = \exp\left(\frac{-\lambda t}{2}\right) \left[\cosh\left(\frac{dt}{2}\right) + \frac{\lambda}{d} \sinh\left(\frac{dt}{2}\right) \right] \quad (\text{S58})$$

where $d = \sqrt{\lambda^2 - 2\gamma_0\lambda}$.

Here, we consider both Markovian dynamics (when $\gamma_0 < \lambda/2$), and non-Markovian dynamics (when $\gamma_0 > \lambda/2$). The corresponding results are shown in Fig. S1 and Fig. S2, respectively.

In the Markovian regime, we choose $\gamma_0 = 0.2\lambda$, the dynamical behaviors of the *QI* REC, the extended coherence, and the local coherence, with respect to different bases are shown in Fig. S1. We simulate the dynamical behaviors of the above coherence measures in different reference bases. In the Markovian regime of the amplitude-damping channels, the *QI* REC and the extended coherence behaves monotonically. However, the local coherence behaves differently in different reference bases; i.e., the monotonicity depends on the choice of reference basis. Note that although the extended coherence of Alice and Bob behaves monotonically in all reference bases in the Markovian regime of the amplitude-damping channel, it cannot be used for detecting non-Markovianity in the general evolution as the case we have experimentally shown in the main text.

In the non-Markovian regime, we choose $\gamma_0 = 25\lambda$, resulting in the non-Markovianity of the open system dynamics. In this case, we simulate both the *QI* REC and the SIC with respect to different bases (as shown in Fig. S2). From the simulation, we can see that during the amplitude-damping channel, the non-Markovianity can be detected with both the *QI* REC and the SIC (note that in the above case the values of the SIC are coincident in all reference bases) independent of the reference basis we choose.

B. Multiple decoherence channels

The dynamics of a single qubit in multiple decoherence channels can be considered for a two-level system with the master equation

$$\frac{d}{dt}\rho_t = \frac{1}{2} \sum_{i=1}^3 \gamma_i(t)(\sigma_i\rho_t\sigma_i - \rho_t), \quad (\text{S59})$$

where σ_i denotes the i th Pauli matrix and γ_i denotes the relaxation rate. The dynamical map corresponding to Eq. (S59) can be exactly worked out and is given by the random unitary dynamics

$$\Lambda_t(\rho) = \sum_{i=0}^3 p_i(t)\sigma_i\rho\sigma_i. \quad (\text{S60})$$

Here, for the Markovian dynamics, we set the parameters $\gamma_i(t)$ as follows

$$\gamma_1(t) = \gamma_2(t) = \gamma_3(t) = \frac{c}{2}, \quad (\text{S61})$$

and for the non-Markovian dynamics, we set the aforementioned parameters as

$$\gamma_1(t) = \gamma_2(t) = \frac{c}{2}, \quad (\text{S62a})$$

$$\gamma_3(t) = \frac{c\lambda \cos ct}{2}, \quad (\text{S62b})$$

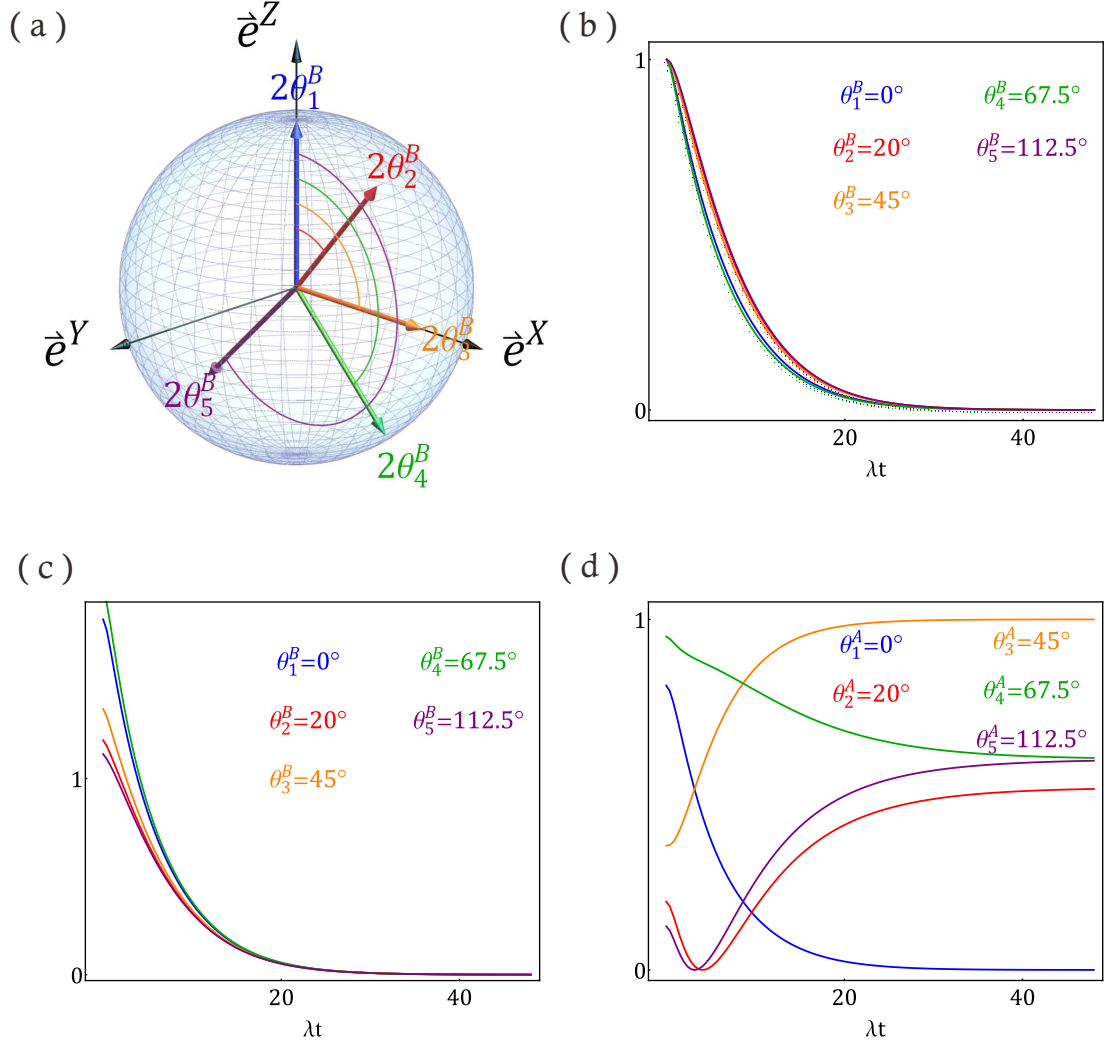


Figure S1. **Theoretical simulations for the Markovian amplitude-damping channels.** In the Markovian regime, the simulations of the dynamical behaviors of the *QI* REC (b), the extended coherence (c), and the local coherence (d) are shown. The reference bases of Alice (Bob) are chosen as the eigenbasis of $\sigma \cdot \mathbf{n}[\theta_i^{A(B)}]$ with different $\theta_i^{A(B)}$, where $\mathbf{n}(\theta_i) = \sin 2\theta_i^x \mathbf{e}^x + \cos 2\theta_i^z \mathbf{e}^z$. During the Markovian evolution, when $\gamma_0 = 0.2\lambda$, both the *QI* REC and the extended coherence of ρ^{AB} decrease monotonically. The dynamical behavior of the local coherence of *A* is non-monotonic and depends on the basis we choose.

where $c > 0$, and $\lambda > 0$, controlling the degree of non-Markovianity.

In the Markovian regime, the dynamics of the system can be exactly solved as

$$p_0(t) = \frac{1 + 3 \exp(-2ct)}{4}, \quad (\text{S63a})$$

$$p_1(t) = p_2(t) = p_3(t) = \frac{1 - \exp(-2ct)}{4}. \quad (\text{S63b})$$

The numerical simulations of the dynamical behaviors of the *QI* REC, the extended coherence, and the local coherence, with respect to different bases (as shown in Fig. S3). In this case, all the above coherence measures behave monotonically during the Markovian dynamics.

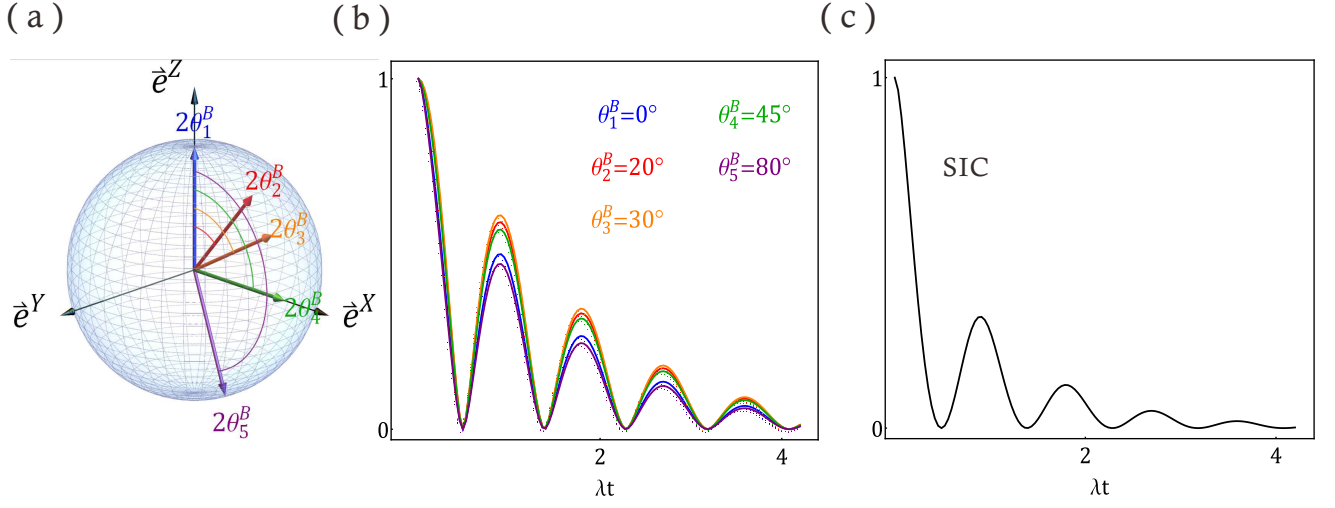


Figure S2. **Theoretical simulations for the non-Markovian amplitude-damping channels.** In the non-Markovian regime, $\gamma_0 = 25\lambda$, the non-Markovianity can be captured by the QI REC (b) and the SIC (c), where the SIC behaves exactly the same in all reference bases, chosen as the eigenbasis of $\sigma \cdot \mathbf{n}(\theta_i^B)$ with different θ_i^B , where $\mathbf{n}(\theta_i^B) = \sin 2\theta_i^B \mathbf{e}^X + \cos 2\theta_i^B \mathbf{e}^Z$.

In the non-Markovian regime, the dynamics of the system can be solved as

$$p_0(t) = \frac{1 + \exp(-2ct) + 2 \exp(-ct - \lambda \sin ct)}{4}, \quad (\text{S64a})$$

$$p_1(t) = p_2(t) = \frac{1 - \exp(-2ct)}{4}, \quad (\text{S64b})$$

$$p_3(t) = \frac{1 + \exp(-2ct) - 2 \exp(-ct - \lambda \sin ct)}{4}. \quad (\text{S64c})$$

We set $\lambda = 3.8$. The dynamical behaviors of the QI REC, and the SIC are simulated with respect to different bases, as shown in Fig. S4. We can see that in all reference bases chosen, the non-Markovianity can be captured by both the temporal increase of the QI REC and the SIC. It should be noticed that our methods cannot capture the non-Markovianity of all parameters of multiple decoherence channels.

S4. NON-MARKOVIANITY MEASURE BASED ON THE QI REC

In this section, we define a new method for non-Markovianity measure based on the QI REC, which is

$$\mathcal{N}_{QI}(\Lambda) = \max_{|i\rangle^B} \int_{\sigma > 0} \sigma(t, |i\rangle^B), \quad (\text{S65})$$

where

$$\sigma(t, |i\rangle^B) = \frac{\partial C_r^{A|B_i}}{\partial t} [\Lambda \otimes \mathbb{I}(|\Phi\rangle\langle\Phi|)], \quad (\text{S66})$$

$C_r^{A|B_i}$ denotes the QI REC with respect to the reference basis $\{|i\rangle^B\}$ of Bob, and $|\Phi\rangle$ can be any pure bipartite maximally entangled state. Thus, this definition only needs optimization over all local bases of Bob's system.

In order to figure out the property of this non-Markovianity measure, let us first recall two popular non-Markovian measures. One was defined by Breuer, Laine, and Piilo (BLP) [10]. A dynamical map $\{\Lambda_t\}$ is Markovian if the distinguishability of any two evolving quantum states ρ and τ decreases, and the associated measure for non-Markovianity measure is then defined as

$$\mathcal{N}_{BLP} = \max_{\rho, \tau} \int_{(\partial\|\rho_t - \tau_t\|/\partial t) > 0} \frac{\partial\|\rho_t - \tau_t\|}{\partial t} dt. \quad (\text{S67})$$

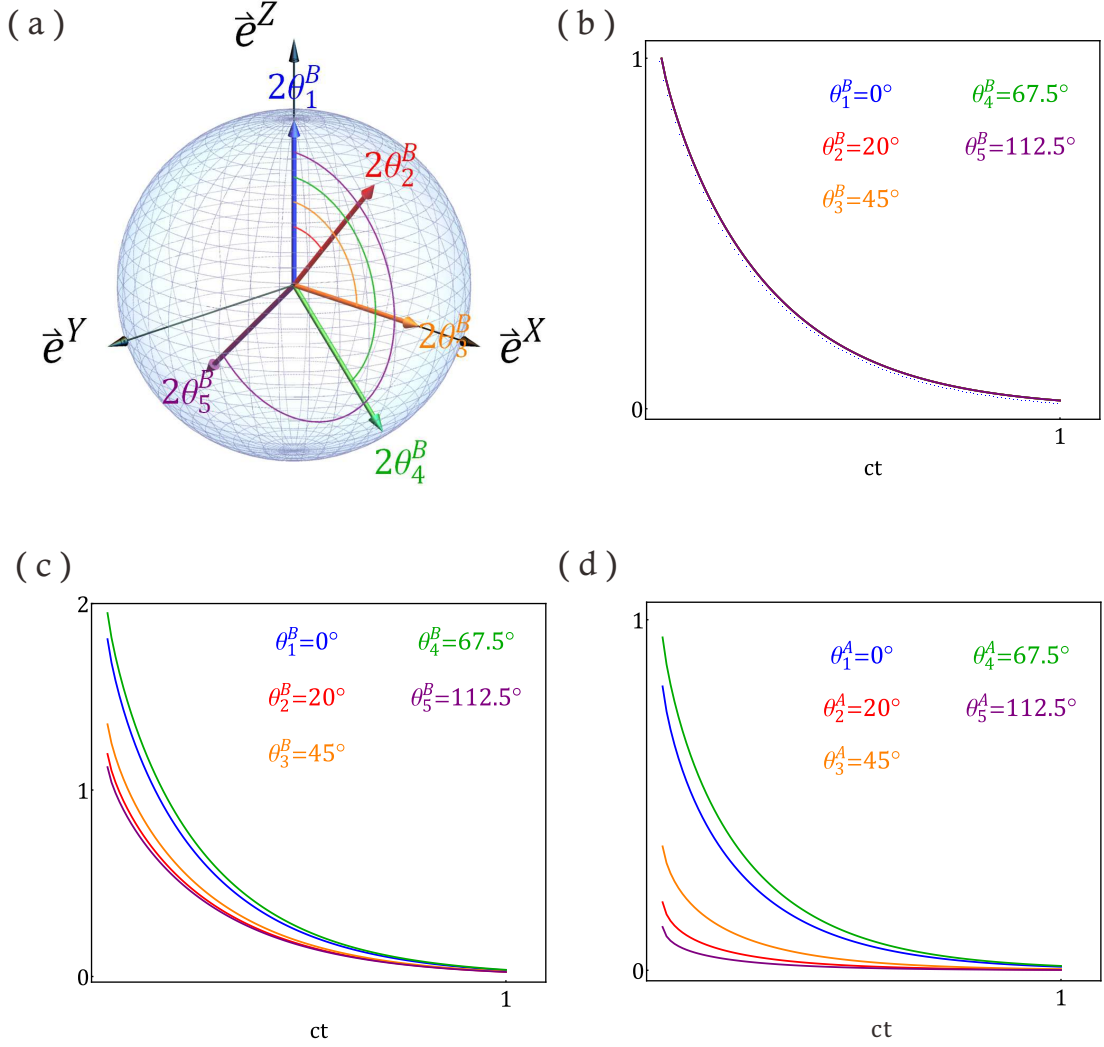


Figure S3. **Theoretical simulations for the Markovian multiple decoherence channels.** In the Markovian regime, the numerical simulations of the dynamical behaviors of the QI REC (b), the extended coherence (c), and the local coherence (d) are shown. The reference basis of Alice (Bob) is chosen as the eigenbasis of $\sigma \cdot \mathbf{n}[\theta_i^{A(B)}]$ with different $\theta_i^{A(B)}$, where $\mathbf{n}(\theta_i^B) = \sin 2\theta_i^B \mathbf{e}^X + \cos 2\theta_i^B \mathbf{e}^Z$. In the Markovian regime, all information quantifiers behave monotonically independent of the basis chosen.

Here ρ and τ denote the initial pairs of quantum states, and $\|\cdot\|$ denotes the trace distance. However, this involves a formidable optimization over all pairs of density operators, which is relatively harder to carry out when working with a high-dimensional system.

The other one was proposed by Rivas, Huelga, and Plenio (RHP) in [11]:

$$\mathcal{N}_{\text{RHP}} = \int_0^\infty \lim_{\varepsilon \rightarrow 0} \frac{\text{Tr}[\Lambda_{t+\varepsilon, t} \otimes \mathbb{I}(|\Phi\rangle\langle\Phi|)] - 1}{\varepsilon} dt \quad (\text{S68})$$

where $|\Phi\rangle$ denotes a maximally entangled state shared by the open system and ancilla. However, this approach needs the computation of the transition map $\Lambda_{t+\varepsilon, t}$, which cannot be evaluated in general. Moreover, an entanglement measure is often difficult to evaluate itself especially in a high-dimensional system.

Another advantage of this method in detecting non-Markovianity is that an initial entanglement or correlations are not necessary. For example, consider an initial state

$$\rho_0^{AB} = \frac{1}{2}|\Phi\rangle\langle\Phi| + \frac{1}{2}|\Psi\rangle\langle\Psi|, \quad (\text{S69})$$

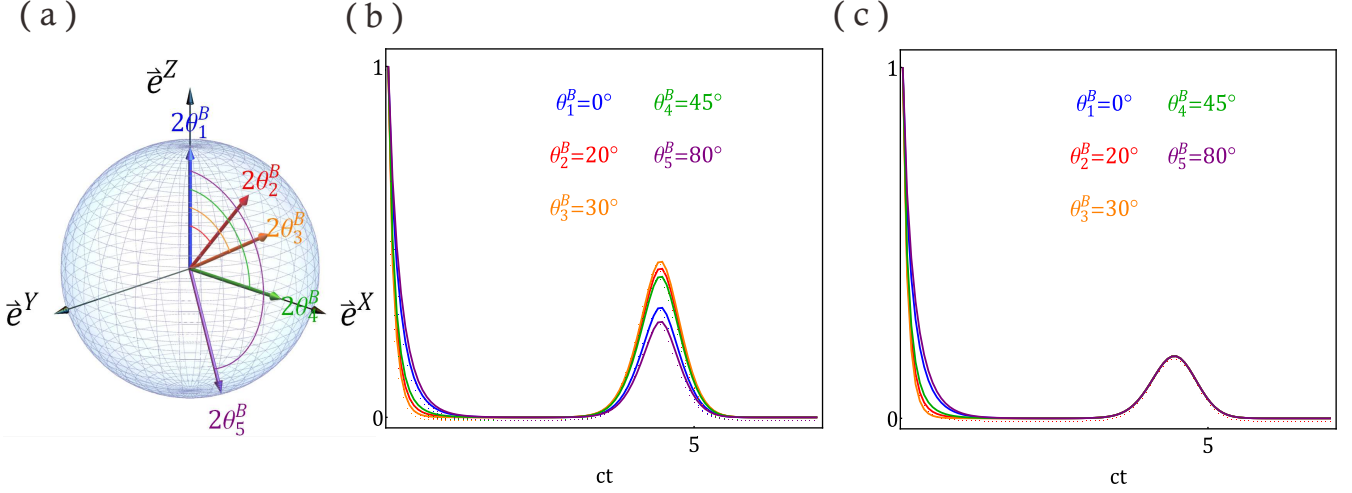


Figure S4. **Theoretical simulations for the non-Markovian multiple decoherence channels.** In the non-Markovian regime, the non-Markovianity can be simultaneously captured by the temporal increase of the *QI REC* (b) and the SIC (c), in all reference bases of Bob, chosen as the eigenbasis of $\sigma \cdot \mathbf{n}(\theta_i^B)$ with different θ_i^B , where $\mathbf{n}(\theta_i^B) = \sin 2\theta_i^B \hat{e}^X + \cos 2\theta_i^B \hat{e}^Z$.

where $|\Phi+\rangle$ and $|\Psi+\rangle$ are Bell states

$$\begin{aligned}
 |\Phi+\rangle &= \frac{1}{\sqrt{2}}(|00\rangle + |11\rangle), \\
 |\Psi+\rangle &= \frac{1}{\sqrt{2}}(|01\rangle + |10\rangle).
 \end{aligned} \tag{S70}$$

The initial ρ^{AB} has zero entanglement and discord but non-zero *QI REC*, i.e.,

$$E_0^{AB}(\rho_0^{AB}) = D_0^{AB}(\rho_0^{AB}) = 0, C_r^{AB}(\rho_0^{AB}) = 1. \tag{S71}$$

Considering the dynamics in our experiments, the behavior of entanglement or discord is rather trivial and we will not observe the non-Markovianity-induced temporal increase of these quantities. However, we can observe an increase in the *QI REC* when the dynamics is not CP divisible. Thus we can use these states for detecting non-Markovianity via *QI REC*.

S5. EXPERIMENTAL ASPECTS

A. State preparation

In the state preparation module (I), two type-I phase-matched β -barium borate (BBO) crystals, whose optical axes are normal to each other, are pumped by a continuous-wave Ar⁺ laser at 351.1 nm, with a power of around 50 mW, for the generation of photon pairs with a central wavelength at $\lambda=702.2$ nm via a *spontaneous parametric down-conversion process* (SPDC). A half-wave plate working at 351.1 nm set before the lens and BBO crystals is used to control the polarization of the pump laser. The two polarization-entangled photons are then separately distributed through two single-mode fibers (SMF), where one represents Bob and the other Alice. Two interference filters with a 4 nm *full width at half maximum* (FWHM) are placed to filter out proper transmission peaks. HWPs at both ends of the SMFs are used to control the polarization of both photons. A quarter-wave plate in Bob's arm is used to compensate the phase for the desired prepared state. A Fabry-Pérot cavity which is 0.06 mm thick and coated with a partial reflecting coating on each side at 702.2 nm (actually the experimental accessible FP cavity is coated with a reflectivity of around 0.85 of both sides at 780 nm, which is close to the value of the reflectivity at 702.2 nm) can be inserted into Alice's arm to change her initial environment. The setup can generate arbitrary pure bipartite states

$$|\Psi^{AB}\rangle = |\psi(\theta)\rangle^{AB} \otimes |\chi\rangle^A, \tag{S72}$$

where $|\psi(\theta)\rangle^{AB}$ denotes the entangled pure states shared by Alice and Bob,

$$|\psi(\theta)\rangle^{AB} = \cos 2\theta|00\rangle + \sin 2\theta|11\rangle, \quad (S73)$$

with arbitrary tunable θ , and $0 \equiv H$, $1 \equiv V$, representing an incoherent basis. The maximally entangled state $|\psi(\frac{\pi}{8})\rangle$ can be prepared with a fidelity of 0.985, with an interference visibility $C_{DD} : C_{DA} \gtrsim 100$, where C_{DD} (C_{DA}) denotes coincident events when Alice is in the state $|D\rangle = \frac{1}{\sqrt{2}}(|0\rangle + |1\rangle)$ and Bob is in the state $|D\rangle$ [$|A\rangle = \frac{1}{\sqrt{2}}(|0\rangle - |1\rangle)$]. The environmental state can be expressed as

$$|\chi\rangle^A = \int \mathbf{d}\omega f(\omega)|\omega\rangle, \quad (S74)$$

which involves the amplitude $f(\omega)$ for Alice's photon in a mode with frequency ω [12].

B. Evolution

In the evolution module (II), all plates (QPs, QWPs and HWPs) are mounted on rotation frames that allow us to construct a dephasing process in an arbitrary orthogonal basis,

$$|n_+(\alpha)\rangle = \cos \alpha|0\rangle + \sin \alpha|1\rangle, \quad (S75a)$$

$$|n_-(\alpha)\rangle = -\sin \alpha|0\rangle + \cos \alpha|1\rangle, \quad (S75b)$$

where α depends on the angle of the optical axis of the QPs. A QWP (rotation angle set to α) in Alice's arm is used for phase compensation between the $|n_+(\alpha)\rangle$ and $|n_-(\alpha)\rangle$ polarized photons. The experimental evolution admits a simple theoretical analysis which is described by a unitary transformation

$$|n_{\pm}(\alpha)\rangle \otimes |\omega\rangle \xrightarrow{U(\alpha)} \exp(-in_{\pm}\omega t)|n_{\pm}(\alpha)\rangle \otimes |\omega\rangle; \quad (S76)$$

the corresponding dynamical map Λ_t takes the form,

$$|n_+(\alpha)\rangle\langle n_+(\alpha)| \xrightarrow{\Lambda_t} |n_+(\alpha)\rangle\langle n_+(\alpha)|, \quad (S77a)$$

$$|n_-(\alpha)\rangle\langle n_-(\alpha)| \xrightarrow{\Lambda_t} |n_-(\alpha)\rangle\langle n_-(\alpha)|, \quad (S77b)$$

$$|n_+(\alpha)\rangle\langle n_-(\alpha)| \xrightarrow{\Lambda_t} \kappa(t)|n_+(\alpha)\rangle\langle n_-(\alpha)|, \quad (S77c)$$

$$|n_-(\alpha)\rangle\langle n_+(\alpha)| \xrightarrow{\Lambda_t} \kappa^*(t)|n_-(\alpha)\rangle\langle n_+(\alpha)|, \quad (S77d)$$

where the decoherence factor reads

$$\kappa(t) = \int \mathbf{d}\omega |f(\omega)|^2 \exp(-i\Delta n\omega t), \quad (S78)$$

and $\Delta n = n_+ - n_-$ denotes the nonzero difference in the refraction indices of the $|n_+(\alpha)\rangle$ and $|n_-(\alpha)\rangle$ polarized photons.

All theoretical simulations are performed considering experimental imperfections, including the experimentally prepared quantum states. For simulating the two aforementioned processes, Λ_t^M and Λ_t^{NM} , for Markovian and non-Markovian dynamics, we made the assumption that in the experiments of the Markovian process, the frequency distribution can be well described with a Gaussian profile with a standard deviation of 6.50×10^{12} Hz (its corresponding FWHM is 3.4 nm). While the non-Markovian process can be well modeled by a sum of two Gaussians centered at two different frequencies, corresponding to wavelengths 700.6 nm and 703.3 nm with amplitudes 0.65 and 0.35.

The essential difficulty in the experiments is the phase compensation for conducting the correct evolution. In the first part of the experiments, the Markovian evolution is constructed as pure dephasing in the eigenbasis $\{|n_+(20^\circ)\rangle, |n_-(20^\circ)\rangle\}$ of $\sigma \cdot \mathbf{n}_0$, where $\mathbf{n}_0 = \cos 40^\circ \mathbf{e}^X + \sin 40^\circ \mathbf{e}^Z$. Hence, we rotate all QPs to 20° . In the ideal case, we assume that no additional phase is introduced between $|n_+(20^\circ)\rangle$ and $|n_-(20^\circ)\rangle$. However, in our experiments, an additional phase $\phi(t)$ will be introduced and the evolution of the extended coherence and the local coherence will behave differently depending on the additional phase $\phi(t)$. For solving this problem, we insert a QWP with rotation angle 20° to compensate the phase, removing $\phi(t)$. As we take experimental data using QPs with different lengths for each evolution time t , the phase compensation is performed each time when we change the lengths of the QPs. In the experiments with the non-Markovian process, since the dynamical behavior of neither the local coherence nor the extended coherence is taken into consideration, the additional phase will not play an important role in the experimental errors. Thus, the *QI* REC is more robust to phase errors in our protocols.

C. State tomography and coherence detection

In the detection module (III), the extinction ratio of the reflected arm of a PBS is lower than the transmissive arm. For improving the extinction ratio, we use a HWP with rotation angle set to 45° and another PBS placed in the reflected arm, resulting in an increase in the extinction ratio. Thus the precision of the tomography process can be improved.

We use multi-mode fibers for directing photons from the free space to the detectors. The use of multi-mode fibers can increase and stabilize the collection efficiency of the photons. The power of the 351.1 nm continuous laser is set to about 50 mW, and the coincidence window is set at 4 ns, resulting in around 1000 coincident events in one second.

The overall quantum state can be reconstructed via the combination of four wave plates (two HWPs and two QWPs) and two PBSs, performing a standard two-qubit state tomography. The state of a single system can also be analyzed via two wave plates and one PBS on Alice's side, while Bob's photons are used as the trigger. Then the coherence-related measures can be calculated directly from the experimentally reconstructed quantum states $\tilde{\rho}$.

* gyxiang@ustc.edu.cn

- [1] T. Baumgratz, M. Cramer, and M. B. Plenio, *Phys. Rev. Lett.* **113**, 140401 (2014).
- [2] E. Chitambar, A. Streltsov, S. Rana, M. N. Bera, G. Adesso, and M. Lewenstein, *Phys. Rev. Lett.* **116**, 070402 (2016).
- [3] A. Winter and D. Yang, *Phys. Rev. Lett.* **116**, 120404 (2016).
- [4] V. Vedral, *Rev. Mod. Phys.* **74**, 197 (2002).
- [5] V. Vedral and M. B. Plenio, *Phys. Rev. A* **57**, 1619 (1998).
- [6] H. Ollivier and W. H. Zurek, *Phys. Rev. Lett.* **88**, 017901 (2001).
- [7] L. Henderson and V. Vedral, *J. Phys. A* **34**, 6899 (2001).
- [8] K. Modi, A. Brodutch, H. Cable, T. Paterek, and V. Vedral, *Rev. Mod. Phys.* **84**, 1655 (2012).
- [9] Z. He, H.-S. Zeng, Y. Li, Q. Wang, and C. Yao, *Phys. Rev. A* **96**, 022106 (2017).
- [10] H.-P. Breuer, E.-M. Laine, and J. Piilo, *Phys. Rev. Lett.* **103**, 210401 (2009).
- [11] A. Rivas, S. F. Huelga, and M. B. Plenio, *Phys. Rev. Lett.* **105**, 050403 (2010).
- [12] B.-H. Liu, L. Li, Y.-F. Huang, C.-F. Li, G.-C. Guo, E.-M. Laine, H.-P. Breuer, and J. Piilo, *Nat. Phys.* **7**, 931 (2011).